JTTEES 1: 161-168

Structure and Properties of Plasma-Sprayed Sialon Coatings

S. Sodeoka, K. Ueno, Y. Hagiwara, and S. Kose

â'-Sialon ($Si_{6-z}Al_zO_zN_{8-z}$, where z = 1, 2, 3, or 4) was plasma sprayed in air, and the structure and properties of the coating were evaluated. Coatings of the Sialon could be produced when z = 3 or 4, whereas coatings were hardly formed for Sialon with z = 1 and 2. The relative density and the Vickers hardness of the Sialon coatings (z = 3 and 4) increased with an increase in plasma power. Elemental analysis and X-ray diffractometry revealed that Sialon partially decomposed during thermal spraying. Nitrogen gas addition to the secondary plasma gas was effective in suppressing this decomposition.

1. Introduction

SIALON is a general term for the oxynitride ceramics composed of Si, Al, O, and N. Many compounds exist in the Si_3N_4-AlN-Al_2O_3-SiO_2 phase diagram,[1] as shown in Fig. 1. β'-Sialon is a well-known material that has a wide range of solid solutions with a βSi_3N_4-type crystallographic structure, where aluminum atoms are substituted for silicon atoms and oxygen atoms substitute for nitrogen atoms. The compound has elemental ratios given by the formula $Si_{6-z}Al_zO_zN_{8-z}$ ($0 < z < 4.2$). It has superior oxidation resistance,[1,2] mechanical strength at high temperature,[3] and corrosion resistance against molten metals.[1,4] Many works have been reported for sintered Sialon ceramics, however, few are concerned with the thermal spray coating of Sialon. In this study, we have synthesized β'-Sialon with z values of 1, 2, 3, and 4 and have performed plasma spraying experiments in air. The coating structure and properties were investigated.

Key Words: crystallographic structure, process optimization, nitrogen gas, Sialon decomposition, Sialon coatings

S. Sodeoka, K. Ueno, and **S. Kose,** Government Industrial Research Institute, Glass and Ceramics Department, Osaka, Japan; and **Y. Hagiwara,** Osaka Electronics and Communication University, Osaka, Japan.

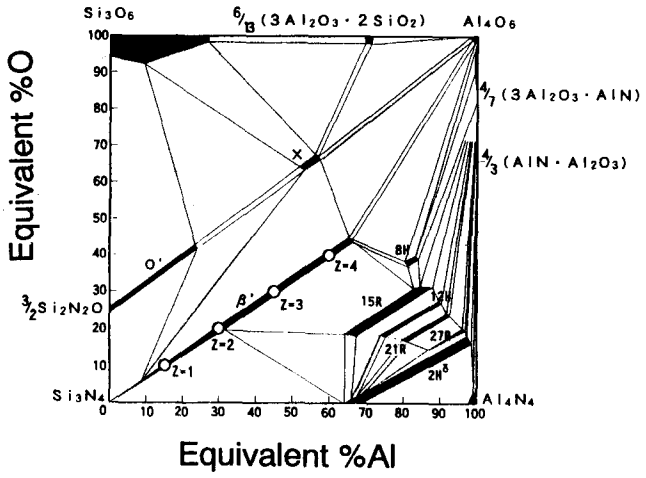

Figure 1 Phase diagram of the Si_3N_4-AlN-Al_2O_3-SiO_2 system.[1]

2. Experimental Procedures

2.1 *Raw Materials*

β'-Sialon was synthesized from commercially available silicon nitride, aluminum oxide, and aluminum nitride powders. Silicon nitride powder, LC-12 grade α-type powder, from Hermann C. Starck was used. The average particle size was 0.55 μm, and the purity was greater than 98%. The aluminum oxide powder was a low-sodium grade from Nikkeikako (grade LS-23, 0.42-μm particle size, greater than 99.8% purity), and the aluminum nitride powder was G grade from Tokuyama Soda (1.7-μm particle size, 98% purity).

Table 1 Blend Proportion of Raw Materials for Each z Value

	Proportion, wt.%		
	Si_3N_4	Al_2O_3	AlN
z = 1	83.06	12.08	4.86
z = 2	66.24	24.08	9.68
z = 3	49.52	36.00	14.47
z = 4	32.91	47.85	19.24

Table 2 Plasma Spraying Parameters

Gun	METCO type 9MB
Plasma gases	
Primary	Ar
Secondary	H_2, H_2 + 49% N_2, H_2 + 90% N_2
Flow rate, l/min	
Primary	37.8 to 41.5
Secondary	7.03 to 10.11
Plasma power, kW	30 to 54 (60 V, 500 to 900 A)
Powder feeder	METCO type 4MP
Powder feed rate, g/min	Approximately 10
Powder carrier gas	Ar
Powder injection	External injector tilted to nozzle
Spraying distance, mm	75

2.2 *Preparation of Spraying Powder*

These powders were stoichiometrically mixed to the desired z value and ball milled in ethyl alcohol. Detailed compositions of the starting powders are given in Table 1 for each z value. After drying, the powder mixtures were molded in a steel die, 40 mm in diameter, and pressed at 19.6 MPa (200 kgf/cm^2). The compacts were fired at 1600 °C for 120 min under a N_2 gas pressure of 0.83 to 0.88 MPa (8.5 to 9.0 kgf/cm^2) in a graphite crucible filled with coarse silicon nitride powder. The Si_3N_4 powder was used to protect the samples against carbon contamination from the graphite crucible. The sintered body was crushed to under 32 μm by planetary ball milling with an alumina pot and balls. Spherically granulated powder was then prepared by spray drying with polyvinyl alcohol as a binder and was classified between 25 and 45 μm for spraying.

z value		1	2	3	4
composition		Si_5AlON_7	$Si_4Al_2O_2N_6$	$Si_3Al_3O_3N_5$	$Si_2Al_4O_4N_4$
Plasma power (kW)	30	—	×	△	○
	42	—	×	○	○
	48	×	△	—	○
	54	×	△	○	○

—:No experiment, ×:No deposit, △:Partial melting, ○:Coating formed

Figure 2 Possibility of thermal sprayed deposition of Sialon materials with z = 1 to 4 at various plasma powers.

2.3 *Plasma Spraying Conditions*

Plasma spraying was carried out with a Perkin-Elmer METCO 9MB gun in air. Argon gas was used as the primary plasma gas and hydrogen or a $H_2 + N_2$ mixture gas was added as the secondary gas. Plasma input power was 30 to 54 kW (60 V, 500 to 900 A), and the spraying distance was 75 mm. Spraying parameters are shown in Table 2.

The substrate was carbon steel (JIS-SS41) that was grit blasted with alumina grit (24-mesh) just prior to spraying. The sprayed coating was formed directly on the substrate without any bond coating. The deposit and substrate were cooled by air blowing to the surface and by a water-cooled specimen holder.

2.4 *Evaluation Methods*

Bulk density of the coating was measured by Archimedes' method, where the free-form deposit is separated from the sub-

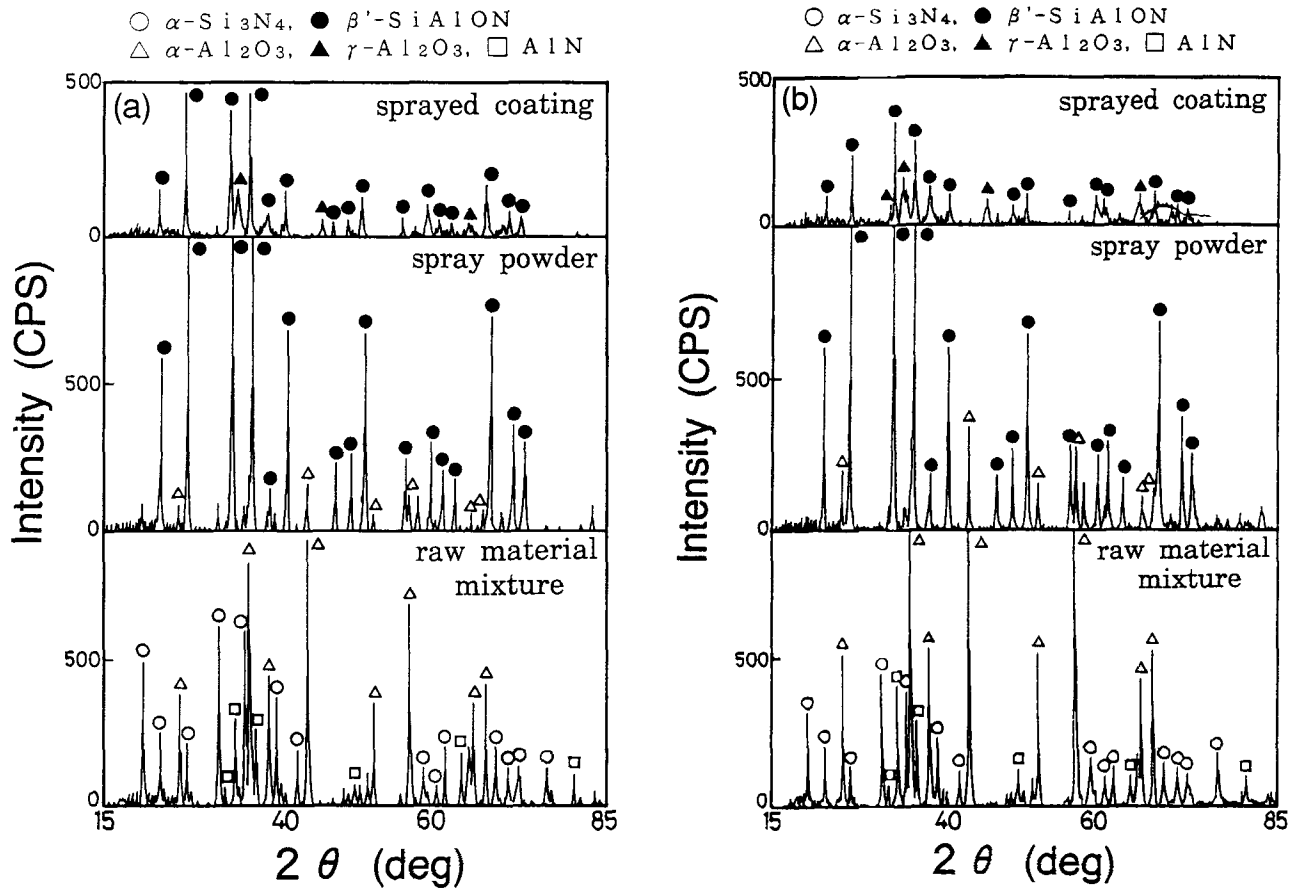

Figure 3 X-ray diffraction patterns of raw material mixture (bottom curve), synthesized powder (middle curve), and sprayed coating at 54 kW (top curve), for Sialon materials with **(a)** z = 3 and **(b)** z = 4, measured with CuKα.

strate by using hydrochloric acid. True density was measured by the pycnometer method after the deposit was pulverized into fine powder. The relative density of the coating was calculated by dividing bulk density by true density. Crystallographic phases were determined for the pulverized sample by the X-ray powder diffraction technique. Nitrogen content was determined by measuring the amount of N_2 gas extracted from the sample, after melting and decomposition in a metal flux, using a Horiba nitrogen-oxygen analyzer,[5] model EMGA-2800. Microstructures of the coatings were observed by scanning electron microscopy (SEM). The distribution of chemical elements was analyzed by energy dispersive X-ray spectroscopy (EPMA). As a mechanical property, Vickers microhardness was measured on the cross section of the deposit.

3. Results and Discussion

3.1 *Structure and Properties of Sialon Coatings*

First, we examined whether Sialon alloys could be thermal sprayed. Sialon alloys with various z values were sprayed at plasma power levels from 30 to 54 kW. In this experiment, the secondary plasma gas was pure hydrogen. The results are shown in Fig. 2, in which an open circle indicates that a reasonably dense deposit was formed on the substrate; an open triangle indicates that the powder was partially melted, but the deposit was crumbly, and the × indicates that no coating was formed.

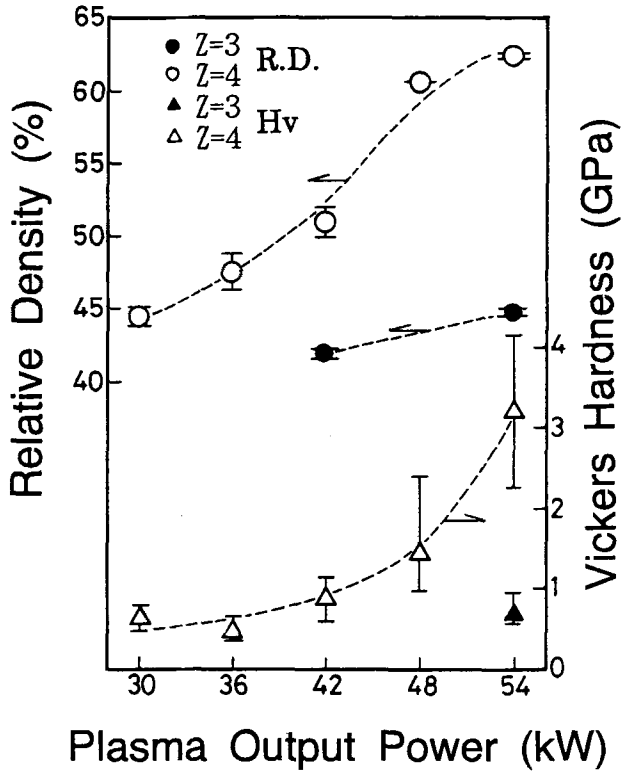

Figure 4 Changes in relative density and Vickers microhardness of the sprayed coating (z = 3 and 4) with plasma power.

Whether Sialon can form a deposit depends on the z value rather than the plasma power. A Sialon with z = 1 produces no deposition at any power level. The Sialon powder with z = 2 was only partially melted, even at high power levels over 48 kW. For z = 3, the Sialon deposit was formed only when the power level was over 42 kW. A Sialon coating was formed at any power level for the Sialon composition with z = 4. Consequently, the higher the z value and/or the plasma power, then the easier a Sialon coating is formed. The results obtained on Sialon compositions with z = 3 and 4 are discussed below.

The X-ray powder diffraction patterns of the raw material mixture, the synthesized spraying powder, and the sprayed deposit with z = 3 and 4 are shown in Fig. 3(a) and (b), respectively. The spraying powder and the deposit were composed of two phases—β′-Sialon and a small amount of alumina. The former was the major component, and no remarkable change was recognized in these charts after atmospheric spraying. For the latter, αAl_2O_3 in the spray powder is considered to be unreacted residue in the synthesis process of Sialon, because its peak positions in the spray powder are close to that of the raw material mixture. After thermal spraying, the structure of alumina changed from α to γ by rapid quenching at the instant of solidification on the substrate. The proportional amount of the alumina increased after spraying, when the peak heights of the alumina were compared to those of the Sialon. These results suggest that partial thermal decomposition of Sialon occurred during spraying.

Figure 4 shows the changes of relative density and microhardness of the Sialon coatings with z = 3 and 4 for the plasma power. The hardness was measured on the polished cross section by using a Vickers indenter with a load of 0.98 to 2.94 N for 30 sec. The density and the hardness of the coatings with z = 3 were both lower than those of the coating with z = 4. It is not surprising because Sialon compositions with z = 4 melt more easily than the material with z = 3, as pointed out previously in this article. The relative density of the coating with z = 4 increased with increasing plasma power. The maximum value was 62.5%, indicating that the deposit was not as dense as other plasma-sprayed ceramic coatings. The hardness also increased with increasing plasma power, corresponding to the increase in density.

Figures 5(a), (b), and (c) show the polished cross sections of the Sialon with z = 4 sprayed at 36, 48, and 54 kW, respectively. Corresponding with the relative density shown in Fig. 4, the apparent porosity decreased as the power increased, but coarse pores remained even in the coating sprayed at 54 kW.

Elemental distribution of aluminum and silicon was evaluated by EPMA on the polished coating. The examined plane was perpendicular to the spraying direction. Figure 6 shows the results for one sample of Sialon with z = 4 sprayed at 54 kW. Here, elemental analysis was carried out on the areas enclosed in white rectangles in the micrographs. The numerical values under each photograph indicate the atomic ratio of silicon and aluminum, calibrated by the usual ZAF method. The equivalent percentages of aluminum atoms obtained for the analyzed areas of (a) through (e) in Fig. 6 are indicated in the phase diagram shown in Fig. 6(f). These results suggest that the Sialon coating is not homogeneous in its composition. Each grain was composed of different proportions of elements. These compositional changes from the feedstock material after thermal spraying could be at-

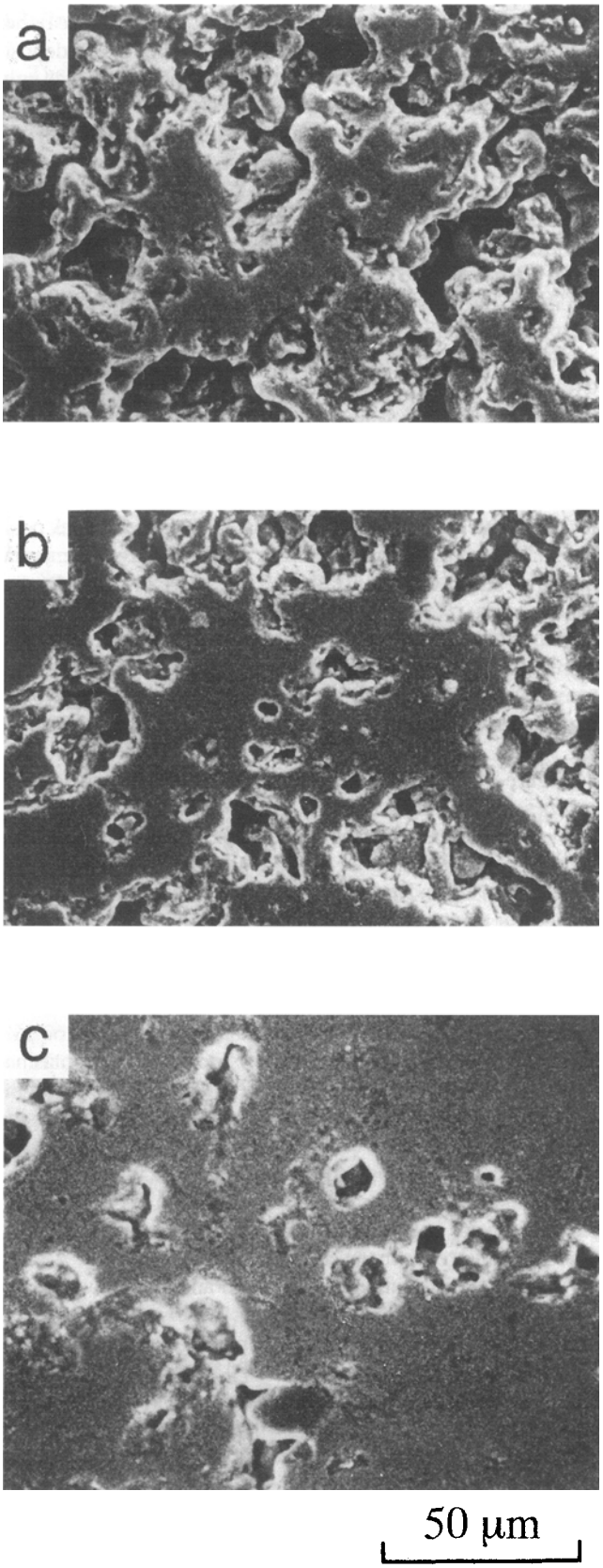

Figure 5 Scanning electron micrograph of the cross section of the $z = 4$ Sialon coatings at various plasma powers. (**a**) 36 kW. (**b**) 48 kW. (**c**) 54 kW.

tributed to thermal decomposition of the material. It is notable that the particles having higher amounts of aluminum seem to be fused better than those with lower atomic percentages (Fig. 6a and 6b).

3.2 *Influence of N_2 Gas on the Decomposition of Sialon*

We considered that the increase in alumina after spraying was due to decomposition of Sialon at high temperatures in the plasma flame. Nitrogen can suppress the decomposition of silicon nitride at high temperatures.[6] Consequently, nitrogen gas addition to the secondary plasma gas was studied to suppress the decomposition of Sialon during plasma spraying.

Figure 7 shows the nitrogen contents in the Sialon ($z = 4$) coatings produced with various secondary gas compositions and plasma power levels. Here, the open triangles indicate composition of the feedstock and correspond well to the estimated value from the blended proportion of raw materials before synthesis. The starting powder contained 20 wt.% nitrogen, but the nitrogen content decreased to about 15 wt.% after spraying with 100% H_2. Addition of N_2 in the secondary gas significantly suppressed the decrease in nitrogen content. When the plasma power increased, however, the suppressing effect of N_2 gas became less distinct.

The decomposition of Sialon was accompanied by a decrease in nitrogen content and an increase in the amount of alumina. Therefore, the partial decomposition of Sialon follows the reaction described as:

$$A(Si_{6-z}Al_zO_zN_{8-z}) + BO_2 \rightarrow CAl_2O_3 + DSiO_2 + EN_2\uparrow \qquad [1]$$

where the coefficients from A to E are proportional constants. Sialon produces alumina, silica, and nitrogen on reaction with oxygen. Silica should produce a glassy phase, because silicon-containing phases other than Sialon were found in the X-ray diffraction pattern. The silicon-rich particle in Fig. 6(a) may correspond to this product, because it has been reported that SiO_2 with a certain amount of Al_2O_3 could form a glass phase after flame spraying.[7,8] Equation 1 also presents an explanation for the suppression of decomposition by the addition of nitrogen gas. Thus, an increase of N_2 pressure restrains the reaction toward the right side.

Hasegawa *et al.*[9] reported that the reaction products of Sialon during long-term oxidation tests were mullite, silica, and nitrogen. Contrary to this result, no mullite, but only an increase in alumina content was found in the coating. The fused phase containing Al_2O_3 and SiO_2 did not form mullite, but a glassy phase and alumina due to the rapid quench on deposition. Owing to the incomplete reaction in Sialon synthesis, the spraying powder contained a small amount of alpha alumina, which acts as a nucleus for grain growth during cooling. The existence of such nuclei may explain why the alumina content increases after spraying.

Figures 8(a) and (b) show the relative densities of the coatings sprayed with various hydrogen gas contents and plasma powers for Sialon materials with $z = 3$ and 4, respectively. The density increased with an increase in the plasma power at all secondary plasma gas compositions. The addition of nitrogen in the plasma gas was found to be effective in increasing the density of the coatings during thermal spraying.

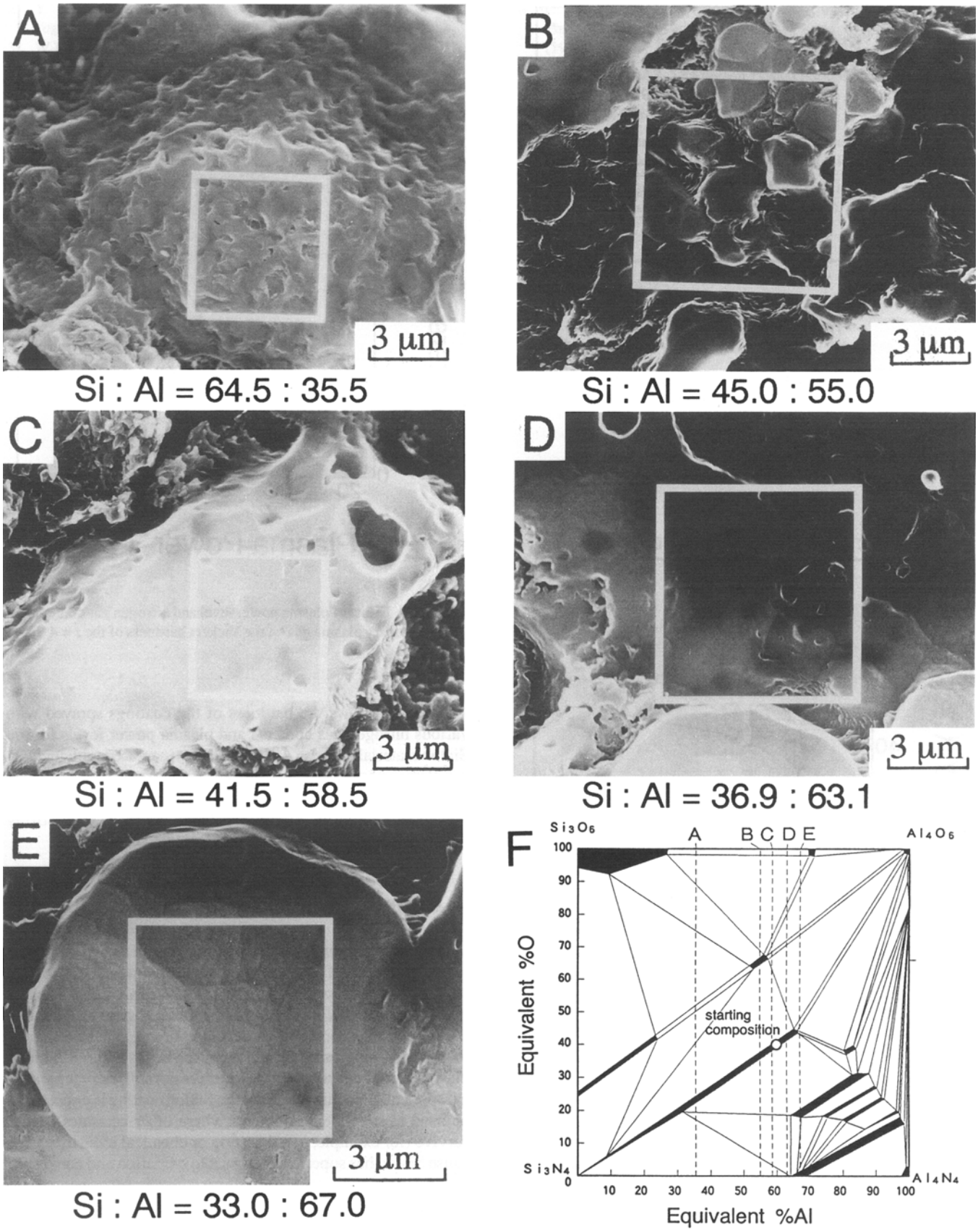

Figure 6 Surface morphology and metallic element proportion of deposited particles sprayed at 54 kW with $z = 4$ Sialon powder. **(a)** through **(e)** illustrate EPMA results on the indicated regions of the coatings. **(f)** shows the relation of these regions to the Sialon phase diagram.

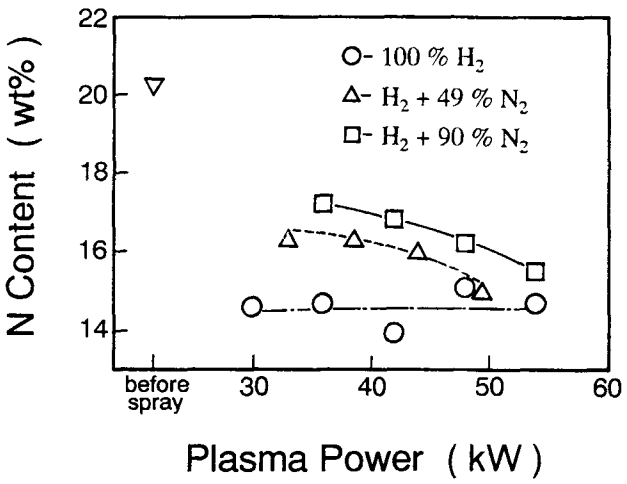

Figure 7 Relationships among nitrogen content in the Sialon (z = 4) coatings, plasma power level, and nitrogen gas content in secondary plasma gas.

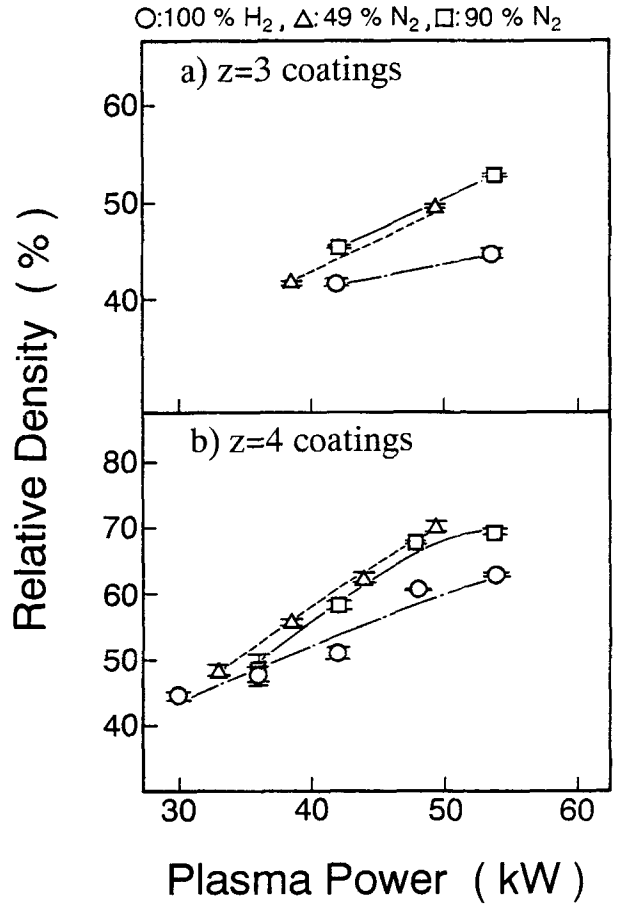

Figure 8 Effect of plasma power level and nitrogen gas content in the secondary plasma gas on the relative density of Sialon coatings. **(a)** z = 3. **(b)** z = 4.

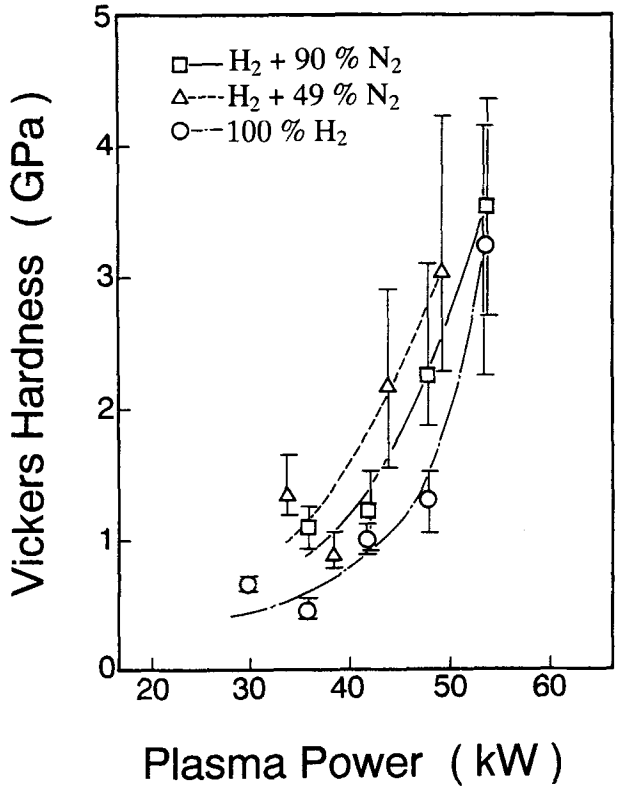

Figure 9 Effect of plasma power level and nitrogen gas content in the secondary plasma gas on the Vickers hardness of the z = 4 Sialon coatings.

Figure 9 shows the hardness of the coatings sprayed with various nitrogen gas contents and plasma power levels for the Sialon material with z = 4. The hardness increased with increasing plasma power. These results suggest a strong correlation between hardness and density. The maximum hardness recorded was about 4.3 GPa (439 kgf/mm^2), being rather lower (probably due to residual porosity) than that of sintered ceramics.

4. Conclusions

Thermal spraying of Sialon materials with z = 1, 2, 3, and 4 was attempted, and coatings with z = 3 and 4 were obtained under atmospheric conditions. The relative density and Vickers hardness increased with increasing plasma power. Although Sialon partially decomposes during spraying, the decomposition may be suppressed by adding nitrogen gas in the secondary plasma gas. The density and hardness is not sufficient for practical application in this stage, but the Sialon coating is expected to be used in severe environments where other ceramics cannot survive (for example, metal casting or chemical industries), because Sialon has superior resistance to oxidation and corrosion.

References

1. K.H. Jack, "Sialons and Related Nitrogen Ceramics," *J. Mater. Sci.*, *11*(6), 1135-1158 (1976).

2. Y. Oyama, "Solid Solution in the System Si_3N_4-AlN-Al_2O_3," *Yogyo-Kyokai-Shi*, *82*(6), 351-357 (1974).
3. W.J. Arrol, The Sialons-Properties and Fabrication, in *Ceramics for High Performance Applications*, J.J. Burke, A.E. Gorum, and R.N. Katz., Ed., Brook Hill Publishing Co., Chestnut Hill, 729-738 (1974).
4. K. Terao, T. Suzuki, and T. Arahori, "Erosion Resistance of Sialon to Stainless Steel," *Yogyo-Kyokai-Shi*, *94*(1), 111-115 (1986) in Japanese.
5. K. Ban and T. Yamada, "Analysis of Oxygen and Nitrogen for Ceramics," *Kinzoku*, *57*(7), 73-76 (1987).
6. C. Greskovich and S. Prochazka, "Stability of Si_3N_4 and Liquid Phase(s) During Sintering," *J. Am. Ceram. Soc.*, *64*(7), C96-97 (1981).
7. M.S.J. Gani and R. McPherson, "Glass Formation and Phase Transformations in Plasma Prepared Al_2O_3-SiO_2 Powders," *J. Mater. Sci.*, *12*(5), 999-1009 (1977).
8. T. Takamori and R. Roy, "Rapid Crystallization of SiO_2-Al_2O_3 Glasses," *J. Am. Ceram. Soc.*, *56*(12), 639-644 (1973).
9. Y. Hasegawa and K. Hirota, "Oxidation Resistance of Silicate Ceramics," *Ceram. Jpn.*, *18*(7), 580-585 (1983).